A tidal breathing model for the multiple inert gas elimination technique

J. P. WHITELEY,[1,2] D. J. GAVAGHAN,[1,2] AND C. E. W. HAHN[1]
[1]Nuffield Department of Anaesthetics, University of Oxford, Radcliffe Infirmary, Oxford OX2 6HE; and [2]Oxford University Computing Laboratory, Oxford OX1 3QD, United Kingdom

Whiteley, J. P., D. J. Gavaghan, and C. E. W. Hahn. A tidal breathing model for the multiple inert gas elimination technique. *J. Appl. Physiol.* 87(1): 161–169, 1999.—The tidal breathing lung model described for the sine-wave technique (D. J. Gavaghan and C. E. W. Hahn. *Respir. Physiol.* 106: 209–221, 1996) is generalized to continuous ventilation-perfusion and ventilation-volume distributions. This tidal breathing model is then applied to the multiple inert gas elimination technique (P. D. Wagner, H. A. Saltzman, and J. B. West. *J. Appl. Physiol.* 36: 588–599, 1974). The conservation of mass equations are solved, and it is shown that *1)* retentions vary considerably over the course of a breath, *2)* the retentions are dependent on alveolar volume, and *3)* the retentions depend only weakly on the width of the ventilation-volume distribution. Simulated experimental data with a unimodal ventilation-perfusion distribution are inserted into the parameter recovery model for a lung with 1 or 2 alveolar compartments and for a lung with 50 compartments. The parameters recovered using both models are dependent on the time interval over which the blood sample is taken. For best results, the blood sample should be drawn over several breath cycles.

ventilation-perfusion; ventilation-volume; gas exchange

INERT GAS TECHNIQUES, such as the multiple inert gas elimination technique (MIGET), have long been used as a tool for investigating the matching of ventilation and perfusion in the lungs. In this technique a subject is infused intravenously with a selection of inert tracer gases, usually six, so that the mixed venous content of these gases is constant. The gases are inert, and the blood content (C) is related to the partial pressure (P) by C = λP, where λ is the Ostwald partition coefficient. The six gases are chosen so that their partition coefficients are approximately evenly spaced on a logarithmic scale. A typical choice of the gas of lowest solubility is sulfur hexafluoride ($\lambda = 5.99 \times 10^{-3}$); a typical choice of the most soluble gas is acetone ($\lambda = 285$). After a period of time has elapsed, a "steady state" is reached, and the partial pressure of each individual tracer gas in the mixed expired gases and in the arterial blood is assumed to be constant. The ratio of mixed expired partial pressure ($P\bar{E}$) to mixed venous partial pressure $P\bar{v}$ of each tracer gas is known as the excretion; the ratio of arterial partial pressure ($P\bar{a}$) to ($P\bar{v}$) is known as the retention. From the retention and excretion of each gas, predictions may be made about the ventilation-perfusion (V/Q) distribution inside the lung. Initial work by Farhi and Yokoyama (2, 3) used a simple lung model with one alveolar compartment. This was developed by Wagner et al. (11) and Evans and Wagner (1) into a 50-compartment lung model.

Previous work on MIGET has made little reference to the effects of tidal breathing. In particular, we demonstrate that tidal breathing causes variations in $P\bar{a}$ within each breath. These variations will also be dependent on the way in which the ventilation is distributed within the lung, and so, theoretically, MIGET should be dependent on the alveolar ventilation-volume ($\dot{V}A/VA$) distribution as well as the $\dot{V}/\dot{Q}$ distribution. We investigate the magnitude of this effect in this study.

We apply the tidal breathing model described by Gavaghan and Hahn (4) for the forced inspired sine-wave technique to MIGET. We begin by describing the differences in the mathematical modeling. We then proceed to demonstrate that the magnitude of the retentions vary over the time course of each breath and investigate the effect of these variations on a model with one alveolar compartment, as described here, and that used by Evans and Wagner (1). We show that unless the retentions are time averaged, considerable differences in both models are caused by these time-varying retentions and that the $\dot{V}/\dot{Q}$ distributions recovered are very dependent on the point of the breath at which the arterial blood is sampled. For example, some retentions generated using a one-compartment tidal model may be recovered as a bimodal $\dot{V}/\dot{Q}$ distribution for a recovery routine based on a continuous ventilation model. Finally, we investigate the dependency of the retentions on the $\dot{V}A/VA$, distribution. It is shown that the width of the $\dot{V}A/VA$ distribution is only of marginal significance but that the dependency on the total alveolar volume (VA_T) may not be neglected.

For clarity, we consider only unimodal $\dot{V}/\dot{Q}$ distributions, inasmuch as the effects of the time-varying retentions can be demonstrated fully using these distributions only.

MODEL

To study the effects of tidal breathing, it is necessary to give a description of the inspiratory and expiratory processes by defining VA as a function of time over each breath. We follow Gavaghan and Hahn (4) and assume a linear increase in volume on inspiration and an exponential decrease in volume on expiration. If we were to consider a lung with more than one mode of ventilation, volume, and perfusion, then we would also have to consider sequential emptying and filling of the compartments under consideration. It would then be necessary to know the emptying pattern to calculate the $P\bar{E}$, since the gas expired from an alveolar compartment that empties last will be left in the series dead space at the end of expiration and will not be included in the mixed expired gases. For the same reason, the constitution of the dead space gas at the end of expira-

tion is dependent on the emptying pattern of the alveolar units, and similarly the distribution of this dead space gas on inspiration is dependent on the filling pattern of the alveolar compartments. Once these processes had been modeled, the conservation of mass equations would still be dependent on the fraction of the tidal volume associated with each compartment, and so the retentions and excretions would now be dependent on the $\dot{V}A/VA$ distribution as well as the $\dot{V}/\dot{Q}$ distribution. For these reasons, we restrict ourselves to a lung model with unimodal $\dot{V}/\dot{Q}$ and $\dot{V}A/VA$ distributions.

One of the major differences between the tidal breathing model and the continuous breathing model is that tidal breathing takes account of the inspiration of gases left in the dead space at the end of each expiration, and so the partial pressure (PD) of this respired gas must be calculated. This is the first step in calculating the retentions for the tidal model. After this has been done, the conservation of mass equations for the tidal breathing model described by Gavaghan and Hahn (4) may be solved.

Calculation of PD

Discrete compartment models. Initially, we consider only unimodal distributions that are collections of discrete compartments. We assume that there is no sequential emptying and filling of compartments for such unimodal distributions. This is generalized to continuous $\dot{V}A/VA$ and $\dot{V}/\dot{Q}$ distributions in *Continuous distributions of ventilation, perfusion, and volume.* The VA of these compartments [$VA_i(t)$] on an arbitrary breath *j* is given by

$$VA_i(t) = \overline{V}A_i + \frac{VT_i}{TI}(t - t_j) \qquad (1)$$

on inspiration, where VT_i is the tidal volume of *compartment i,* TI is the duration of inspiration, and t_j is the time at the beginning of *breath j;* for expiration

$$VA_i(t) = \overline{V}A_i + VT_i\, e^{-\gamma[t-(t_j+TI)]} \qquad (2)$$

where $\overline{V}A_i$ denotes end-expiratory volume of *compartment i* and γ takes the same value for each lung unit.

The total lung alveolar volume as a function of time [$VA(t)$] and total tidal volume (VT) are related by

$$VA(t) = \sum_{i=1}^{n} VA_i(t) \qquad (3)$$

$$\overline{V}A = \sum_{i=1}^{n} \overline{V}A_i \qquad (4)$$

$$VT = \sum_{i=1}^{n} VT_i \qquad (5)$$

Let the VA_T be $\overline{V}A + VD$ at time TI_D after the beginning of inspiration, where VD is the airway series dead space volume. Then, during the time interval $t_j < t < t_j + TI_D$, the gas entering the alveolar compartment

from the dead space volume will be the gas that was left in the dead space at the end of the previous expiration. At *time* $t = t_j + TI_D$

$$\overline{V}A + VD = \sum_{i=1}^{n}\left(\overline{V}A_i + \frac{VT_i}{TI} TI_D\right)$$

This may be simplified using *Eqs. 3–5* to give

$$TI_D = \frac{VD}{VT}\cdot TI$$

In the time $t_j < t < t_j + TI_D$, the gas left in the dead space will be inspired into the alveolar compartment.

In a similar manner, let the total alveolar volume be $\overline{V}A + VD$ at TE_D after the beginning of expiration. Then, for the remainder of expiration after this time, the gas leaving the alveolar volume will be left in the dead space at the end of expiration. We calculate TE_D by using an argument similar to that used to derive TI_D to give

$$TE_D = \frac{1}{\gamma}\ln\frac{VT}{VD}$$

The gas leaving the alveolar compartment during the time $t_j + TI + TE_D < t < t_{j+1}$ will be the gas that is left in the dead space at the end of expiration. The partial pressure of this gas (PD) may be calculated using

$$PD = \left[\sum_{i=1}^{n}\int_{t_0}^{t_1}\frac{dVA_i}{dt}PA_i(t)dt\right]\left(\sum_{i=1}^{n}\int_{t_0}^{t_1}\frac{dVA_i}{dt}dt\right)^{-1}$$

$$= -\frac{1}{VD}\sum_{i=1}^{n}\int_{t_0}^{t_1}\frac{dVA_i}{dt}PA_i(t)dt \qquad (6)$$

where $t_0 = t_j + TI + TE_D$ and $t_1 = t_{j+1}$. There is a negative sign in front of this integral, because the alveolar volume is decreasing, and so dVA_i/dt is negative.

Continuous distributions of ventilation, perfusion, and volume. The underlying $\dot{V}A/VA$ and $\dot{V}/\dot{Q}$ distributions are often assumed to be log-normal distributions (6, 9). Assuming this to be the case, we now derive an expression for PD for continuous $\dot{V}/\dot{Q}$ and $\dot{V}A/VA$ distributions. Later we will use these continuous distributions to generate theoretical data and compare the competing models. Defining

$$x = \ln\frac{\overline{V}A_d}{VT_d} \qquad y = \ln\frac{VT_d}{\dot{Q}} \qquad (7)$$

where $\overline{V}A_d$ is the alveolar volume distribution and VT_d is the tidal volume distribution at a point in the alveolar compartment. We may also write VT_d as a function of *x* and *y*

$$VT_d(x, y) = A\exp[-(x - \bar{x})^2/2\sigma_x^2]$$
$$\cdot\exp[-(y - \bar{y})^2/2\sigma_y^2] \qquad (8)$$

where $\bar{x}$ and $\bar{y}$ are the mean $\dot{V}A/VA$ and mean $\dot{V}/\dot{Q}$, respectively. This log-normal distribution has a peak at

the point in the (x, y) plane in the region of $(\bar{x}, \bar{y})$ decaying to zero away from this point. The rate of decay is related to the magnitude of σ_x and σ_y, large values giving broad distributions and small values giving narrow distributions. The constant A is found by noting that

$$V_T = \int_{y=-\infty}^{\infty} \int_{x=-\infty}^{\infty} V_{T_d}(x, y) dx\, dy$$

and so

$$A = \frac{V_T}{2\pi\sigma_x\sigma_y} \qquad (9)$$

Equations 7 and *8* enable us to write expressions for the alveolar volume and perfusions as functions of x and y. Using *Eq. 7,* we write

$$\overline{V}_{A_d}(x, y) = \frac{\overline{V}_{A_d}(x, y)}{V_{T_d}(x, y)} V_{T_d}(x, y) = e^x V_{T_d}(x, y) \qquad (10)$$

In a similar way

$$\dot{Q}(x, y) = e^{-y} V_{T_d}(x, y) \qquad (11)$$

The total alveolar volume $(\overline{V}_A)$ may be calculated as follows

$$\overline{V}_A = \int_{y=-\infty}^{\infty} \int_{x=-\infty}^{\infty} \overline{V}_{A_d}(x, y) dx\, dy = V_T e^{\bar{x}} e^{\sigma_x^2/2}$$

Similarly, the pulmonary blood flow is given by

$$\dot{Q}_P = V_T e^{-\bar{y}} e^{\sigma_y^2/2}$$

T_{I_D} and T_{E_D} are calculated in a manner analogous to that described above. We note that the V_{A_T} at *time t* is given for inspiration by

$$V_{A_T}(t) = \int_{y=-\infty}^{\infty} \int_{x=-\infty}^{\infty} \overline{V}_A(x, y) + \overline{V}_T(x, y)(t - t_j) dx\, dy$$

$$= V_{A_T}(t_j) + V_T(t - t_j)$$

We may use the same argument that was used for discrete compartments to show that the time taken for the dead space to be inspired is $(V_D/V_T)T_I$. The same method applied on expiration gives

$$T_{E_D} = \gamma^{-1} \ln(V_T/V_D)$$

We may now define P_D for continuous $\dot{V}/\dot{Q}$ and $\dot{V}_A/V_A$ distributions to be the triple integral

$$P_D = -\frac{1}{V_D} \int_{y=-\infty}^{\infty} \int_{x=-\infty}^{\infty} \int_{t=t_0}^{t=t_1} \frac{\partial V_A(x, y, t)}{\partial t}$$

$$\cdot P_A(x, y, t) dt\, dx\, dy \qquad (12)$$

where $t_0 = t_j + T_I + T_{E_D}$ and $t_1 = t_{j+1}$. We note that there is a minus sign outside the integral to cancel the negative partial derivative of V_A with respect to time. This completes our description of the calculation of P_D.

Retentions and Excretions

Here we demonstrate how to calculate the retentions and excretions. We begin by considering the classical three-compartment lung model, i.e., a lung model consisting of a dead space, a shunt, and a homogeneous alveolar compartment. The governing conservation of mass equations are described by Gavaghan and Hahn (4) for inspiration

$$\frac{d}{dt}[V_A(t)P_A(t)] = \frac{dV_A}{dt} P_{I_A}(t) + \lambda\dot{Q}_P[P_{\bar{v}} - P_A(t)] \quad (13)$$

and for expiration

$$\frac{d}{dt}[V_A(t)P_A(t)] = \frac{dV_A}{dt} P_A(t) + \lambda\dot{Q}_P[P_{\bar{v}} - P_A(t)] \quad (14)$$

where λ is the blood-gas partition coefficient, $\dot{Q}_P$ is the pulmonary blood flow, $P_{\bar{v}}$ is the constant mixed venous partial pressure, and $P_{I_A}(t)$ is the partial pressure of the gas under consideration inspired from the dead space volume, which is given by

$$P_{I_A}(t) = \begin{cases} P_D & t_j < t < t_j + T_{I_D} \\ 0 & t_j + T_{I_D} < t < t_j + T_I \end{cases}$$

where P_D is the partial pressure of the gas in the dead space at the end of expiration, as described in *Eq. 6.* *Equations 13* and *14* are solved numerically using library computer subroutines (7), for N breaths, subject to the initial condition $P_A(0) = 0$. N is chosen large enough so that a breath-by-breath steady state is reached: the partial pressures at onset of inspiration and end of expiration on *breath N* are equal and given by $P_A(t_N)$. *Equations 13* and *14* are then solved on *breath N + 1* to show how $P_A(t)$ varies over the course of one breath in this "pseudo"-steady state.

The retention is the ratio of $P_{\bar{a}}$ to $P_{\bar{v}}$. $P_{\bar{a}}$ is the perfusion-weighted mean of the partial pressure from the alveolar and shunt compartments, given by P_A and $P_{\bar{v}}$, respectively. We see from *Eqs. 13* and *14* that, over the course of each breath, P_A is a function of time and, therefore, so is the retention. We now define the retention to be a function of time as well as solubility, $R(\lambda, t)$, given by

$$R(\lambda, t) = \frac{\dot{Q}_P}{\dot{Q}_T} \frac{P_A(t)}{P_{\bar{v}}} + \frac{\dot{Q}_S}{\dot{Q}_T} \qquad (15)$$

where $\dot{Q}_S$ is the blood flow that bypasses the lung alveolar compartment and $\dot{Q}_T$ is the total blood flow $(\dot{Q}_T = \dot{Q}_P + \dot{Q}_S)$.

In practice, the retentions are measured from a blood sample withdrawn steadily over a period of time. If this sample is taken in the interval $\tau_0 < t < \tau_1$, then the retention is given by

$$R(\lambda, \tau_0, \tau_1) = \frac{\dot{Q}_P}{\dot{Q}_T} \frac{1}{P_{\bar{v}}} \left[\int_{\tau_0}^{\tau_1} P_A(t) dt \right] \left(\int_{\tau_0}^{\tau_1} dt \right)^{-1} + \frac{\dot{Q}_S}{\dot{Q}_T}$$

$$= \frac{\dot{Q}_P}{\dot{Q}_T} \frac{1}{P_{\bar{v}}(\tau_1 - \tau_0)} \int_{\tau_0}^{\tau_1} P_A(t) dt + \frac{\dot{Q}_S}{\dot{Q}_T} \qquad (16)$$

and we note the dependency of the retention on τ_0 and τ_1.

The excretion [$E(\lambda)$] is calculated from the mixed expired gases and so is calculated only once on each breath and is not a function of time once the pseudo-steady state has been reached. The mixed expired gases will contain a volume V_D of gas that was left in the dead space at the end of inspiration and so will contain no tracer gas, together with a volume $V_T - V_D$ of alveolar gas expired between times $t = t_j + T_I$ and $t = t_j + T_I + T_{E_D}$. We may therefore write

$$
\begin{aligned}
E(\lambda) &= \frac{V_T - V_D}{V_T} \left[\int_{t_j+T_I}^{t_j+T_I+T_{E_D}} \frac{dV_A}{dt} \frac{P_A(t)}{P\overline{v}} \, dt \right] \\
&\quad \cdot \left(\int_{t_j+T_I}^{t_j+T_I+T_{E_D}} \frac{dV_A}{dt} \, dt \right)^{-1} \\
&= -\frac{1}{V_T} \int_{t_j+T_I}^{t_j+T_I+T_{E_D}} \frac{dV_A}{dt} \frac{P_A(t)}{P\overline{v}} \, dt
\end{aligned}
\tag{17}
$$

where $V_A(t)$ is defined in *Eq. 2.*

Much previous work on MIGET has used only the retentions in the recovery process (1, 5, 10). As a result, we consider the retentions in much more detail in the remainder of the study.

We may now generalize the calculation of retentions and excretions to continuous $\dot{V}/\dot{Q}$ and $V_A/\dot{V}_A$ distributions. For any values of x and y, *Eqs. 7* and *11* give values of V_T, V_A, and $\dot{Q}$. *Equations 13* and *14* together with the initial condition $P(x, y, 0) = 0$ may then be solved in the same way as for the one-compartment model to give a pseudo-steady-state solution. The retentions as a function of t are now given by the double integral

$$
\begin{aligned}
R(\lambda, t) &= \frac{1}{\dot{Q}_T} \int_{y=-\infty}^{\infty} \int_{x=-\infty}^{\infty} \dot{Q}(x, y) \\
&\quad \cdot \frac{P_A(x, y, t)}{P\overline{v}} \, dx \, dy + \frac{\dot{Q}_S}{\dot{Q}_T}
\end{aligned}
\tag{18}
$$

and the time-averaged retention over the time interval $\tau_0 < t < \tau_1$ is

$$
\begin{aligned}
R(\lambda, \tau_0, \tau_1) &= \frac{1}{\dot{Q}_T(\tau_1 - \tau_0)} \int_{y=-\infty}^{\infty} \int_{x=-\infty}^{\infty} \int_{\tau_0}^{\tau_1} \dot{Q}(x, y) \\
&\quad \cdot \frac{P_A(x, y, t)}{P\overline{v}} \, dt \, dx \, dy + \frac{\dot{Q}_S}{\dot{Q}_T}
\end{aligned}
\tag{19}
$$

The equation corresponding to *Eq. 17* for the excretion is

$$
\begin{aligned}
E(\lambda) &= -\frac{1}{V_T} \int_{y=-\infty}^{\infty} \int_{x=-\infty}^{\infty} \int_{t=t_j+T_I}^{t_j+T_I+T_{E_D}} \\
&\quad \cdot \frac{\partial V_A(x, y, t)}{\partial t} \frac{P_A(x, y, t)}{P\overline{v}} \, dt \, dx \, dy
\end{aligned}
\tag{20}
$$

Parameter Recovery

To evaluate the validity of the steady-state model, retentions will be generated using the tidal breathing model, which we will term the "given data." These data will then be substituted into the parameter recovery routines for a 1- and a 50-compartment model, and the parameters recovered will be compared with the parameters used to generate the data. Changing to the more complex tidal breathing model will affect only the given retentions. Because we use an identical recovery procedure, the effect of experimental error will be identical to those described by Ratner and Wagner (8). We do not therefore consider the effect of experimental error.

One-compartment model. We use the classical one-alveolar-compartment model together with a dead space and shunt compartment, derived by using one alveolar compartment in the model used by Wagner et al. (11). Given shunt fraction ($\dot{Q}_S/\dot{Q}_T$) and $\dot{V}/\dot{Q}$ for the alveolar compartments, we may calculate the retentions (R_i^c) for a given set of gases. Given a set of retentions (R_i), we allow $\dot{Q}_S/\dot{Q}_T$ and $\dot{V}/\dot{Q}$ to vary and minimize

$$
\sum (R_i - R_i^c)^2
$$

subject to $\dot{Q}_S/\dot{Q}_T$ and $\dot{V}/\dot{Q}$ being nonnegative.

Fifty-compartment model. The recovery routine used for the 50-compartment model was identical to that used by Evans and Wagner (1).

RESULTS

Variation of Retentions Within Each Breath

As previously pointed out, $R(\lambda, t)$ varies over the course of each breath, and a typical variation in R is illustrated in Fig. 1 for a single breath lasting 5 s (inspiration of 1.5 s and expiration of 3.5 s). $R(\lambda, t)$ is calculated using the tidal breathing model with continuous $\dot{V}/\dot{Q}$ and $V_A/\dot{V}_A$ distributions by using *Eqs. 13, 14,* and *18.* V_T was 700 ml, V_D was 150 ml, respiratory rate was 12 breaths/min, and shunt was zero. The values of σ_x and σ_y, defined in *Eq. 8,* were both 0.5, and the means of these distributions were chosen so that end-expiratory V_A was 2,380 ml and $\dot{Q}_P$ was 5.95 l/min. $R(\lambda, t)$ is plotted for each of the six values of λ typically used in practice, as shown in Table 1. The retention of enflurane ($\lambda = 2.34$) over the course of five individual breaths is shown with an expanded y-axis in Fig. 2. There are three distinct sections to the variation in retention over the time course of each breath. First, the gas left in the dead space at the end of the previous expiration is inspired: the partial pressure of the gas under consideration in this dead space gas is very similar to that of the gas inside the alveolar compartment, and so the partial pressure inside the alveolar compartment is largely unchanged. In the next section, gas inspired externally enters the alveolar compartment. This gas contains no tracer gas, and so the partial pressure of the tracer gas inside the alveolar compartment decreases through dilution. Expiration is the third section. During this phase, the alveolar partial pressure rises to the value at the start of inspiration.

In Fig. 1, over the course of a breath, some of the retentions vary by ~20%. We would therefore expect any parameter recovery process to be dependent on the exact time within the breath that the arterial blood is

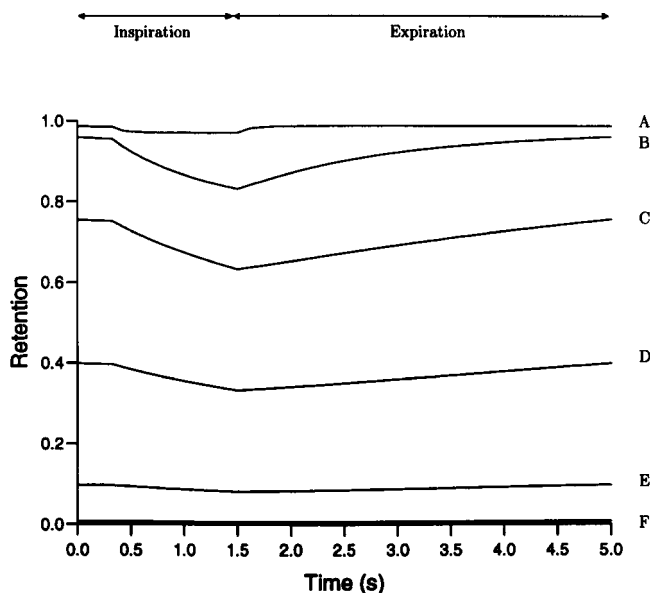Fig. 1. Variation in retentions in time over course of 1 breath. Lines correspond to gases in Table 1: acetone (*A*), ether (*B*), enflurane (*C*), cyclopropane (*D*), ethane (*E*), and sulfur hexafluoride (*F*). Inspiratory time is 1.5 s; expiratory time is 1.5 s, and respiratory rate is, therefore, 12 breaths/min. Flat part of retention plot at beginning of inspiration is due to dead space that is inspired before fresh gas reaches alveoli.

sampled. We consider this further when we substitute the simulated data into the parameter recovery procedure.

For the 50-compartment model, gases with low solubilities (and, therefore, low retentions) give the most information about compartments with low $\dot{V}/\dot{Q}$ ratios; gases with high retentions give information about compartments with high $\dot{V}/\dot{Q}$ ratios. The second- and third-highest retentions vary the most in Fig. 1. By recovering distributions with use of the 50-compartment model (incorporating the continuous ventilation assumption) by using retentions taken from different stages of the breath, we would therefore expect compartments with a high $\dot{V}/\dot{Q}$ ratio to be altered most.

Effect of $\dot{V}_A/V_A$ on Retentions

As we stated earlier, the conservation of mass equations, *Eqs. 13* and *14,* are dependent on lung volume and $\dot{V}_A/V_A$ distribution as well as the $\dot{V}/\dot{Q}$ distribution. Here we demonstrate this numerically. First, we use a one-compartment model to show the effect of alveolar volume on the retentions. Then we use continuous $\dot{V}/\dot{Q}$ and $\dot{V}_A/V_A$ distributions to show the effect of width of the distribution on retentions.

Table 1. *Gases and their partition coefficients*

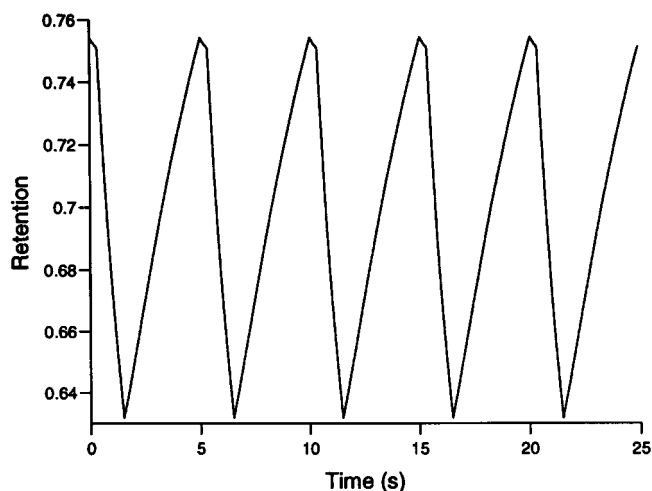| Gas	Partition Coefficient
Sulfur hexafluoride	5.99×10^{-3}
Ethane	8.556×10^{-2}
Cyclopropane	5.348×10^{-1}
Enflurane	2.339
Ether	12.48
Acetone	2.852×10^{2}

Fig. 2. Magnification for data in Fig. 1, *line C,* showing variation in retention of enflurane as a function of time over course of 5 breaths. Trough in retention corresponds to end of inspiration; and peak corresponds to time after start of inspiration when dead space gas (from preceding breath) has been inspired.

Effect of alveolar volume on retentions. We consider six sets of retentions, all calculated using the tidal breathing model, *Eq. 18.* These retentions are generated using the solubilities of the gases typically used, as described by Kapitan and Wagner (5), shown in Table 1. The first three sets are generated using a lung with a unimodal distribution of ventilation, volume, and perfusion. In the notation of *Eq. 8,* $\bar{x} = \ln 3$, $\bar{y} = \ln 6$, and $\sigma_x = \sigma_y = 0.5$. V_T was 500 ml, V_D was 150 ml, shunt was 0, respiratory rate was 12 breaths/min, and breath inspiratory-to-expiratory ratio was 1.5:3.5. This gave $\overline{V}_A$ of 1,700 ml. By measuring the retentions at the point at which they are lowest for each gas in Fig. 1, we obtain one set of retentions (set $R_{1,L}$), and similarly by taking the highest retentions we obtain another set of retentions (set $R_{1,H}$). We may also time average the retentions over the course of a whole breath to give us a third set, $\overline{R}_1$. Three more sets, $R_{2,L}$, $R_{2,H}$, and $\overline{R}_2$, are generated using the same procedure, but this time $\bar{x} = \ln 6$, giving $\overline{V}_A$ of 3,400 ml but otherwise identical lung parameters and respiratory rate. These six sets of retentions are shown in Table 2.

The retentions used in practice are time averaged because of the physical necessity of taking a blood sample. Even so, the alveolar volume at the end of expiration still makes a difference. There are errors of >5% between $\overline{R}_1$ and $\overline{R}_2$. This error is larger than the maximum experimental error expected in measurement of gas concentrations in the blood (10), and so any model that does not take into account $\overline{V}_A$ suffers from modeling errors.

We plot the given distributions and the distributions recovered using the 50-compartment model from the sets of retentions $R_{1,H}$ and $R_{2,H}$ in Fig. 3*A,* the distributions recovered from the sets of retentions $R_{1,L}$ and $R_{2,L}$ in Fig. 3*B,* and the distributions recovered from the sets of retentions $\overline{R}_1$ and $\overline{R}_2$ in Fig. 3*C.* When we use the highest or lowest retentions over the course of a breath, the distributions depend on alveolar volume. However, when the time-averaged retentions are used, as would

Table 2. *Differences in retention caused by doubling alveolar volume*

Partition Coefficient	Retention					
	Set $R_{1,L}$	$R_{1,H}$	Set $\overline{R}_1$	Set $R_{2,L}$	Set $R_{2,H}$	Set $\overline{R}_2$
5.99×10^{-3}	0.0091	0.0108	0.0100	0.0091	0.0100	0.0095
8.56×10^{-2}	0.1129	0.1340	0.1237	0.1136	0.1249	0.1195
5.35×10^{-1}	0.4136	0.4887	0.4530	0.4258	0.4668	0.4477
2.34	0.6981	0.8195	0.7659	0.7284	0.7972	0.7662
12.5	0.8562	0.9693	0.9309	0.8895	0.9634	0.9359
2.85×10^2	0.9713	0.9832	0.9806	0.9774	0.9832	0.9866

In 1st 3 sets of retentions ($R_{1,L}$, $R_{1,H}$, and $\overline{R}_1$), end-expiratory alveolar volume ($\overline{V}_A$) = 1.7 liters; in 2nd 3 sets of retentions ($R_{2,L}$, $R_{2,H}$, and $\overline{R}_2$), $\overline{V}_A$ = 3.4 liters. Subscripts H and L refer to highest and lowest retentions over course of a breath; $\overline{R}_1$ and $\overline{R}_1$ refer to retentions time averaged over a whole breath.

be the case in practice, the distributions do not differ very much.

Effect of the width of the continuous distribution of volume, ventilation, and perfusion. We now consider the effect of the width of the $\dot{V}_A/V_A$ distribution on the generated retentions. As with the one-compartment model, we generate six sets of retentions using *Eqs. 13, 14,* and *18.* The first three sets, $R_{1,L}$, $R_{1,H}$, and $\overline{R}_1$, are generated using a narrow $\dot{V}_A/V_A$ distribution with σ_x = 0.0625. These retentions are the lowest, highest, and time-averaged values of retention over the course of each breath, respectively. The second three sets, $R_{2,L}$, $R_{2,H}$, and $\overline{R}_2$, come from a broad $\dot{V}_A/V_A$ distribution with σ_x = 0.5. The retentions are again the highest, lowest, and time-averaged retentions seen over the course of a breath. Other lung parameters used to generate these retentions were V_T = 500 ml, V_D = 150 ml, $\overline{x}$ = 4.0, $\overline{y}$ = 6.0, and $\dot{Q}_S$ = 0; Respiratory rate was 12 breaths/min. The retentions are shown in Table 3.

For the retentions shown in Table 3, we see that, by comparing the lowest retentions (sets $R_{1,L}$ and $R_{2,L}$), the highest retentions (sets $R_{1,H}$ and $R_{2,H}$), and the time-averaged retentions (sets $\overline{R}_1$ and $\overline{R}_2$), the width of the $\dot{V}_A/V_A$ distribution, when varied from a very narrow to a very broad distribution, makes very little difference in comparison, for example, to the effect of alveolar volume shown in Table 2. Therefore, the width of the $\dot{V}_A/V_A$ distribution is not a major factor in the retentions measured in practice.

Parameter Recovery

Here we investigate the effects of using tidally generated retentions with the previously described parameter recovery methods. We generated two sets of theoretical data using the continuous $\dot{V}_A/V_A$ and $\dot{V}/\dot{Q}$ distributions described earlier (*Eqs. 13, 14,* and *18.* Both had V_T = 700 ml, $\sigma_x = \sigma_y$ = 0.5, and $\overline{x}$ = ln 3. This gave V_A = 2,380 ml. The first case considered had $\overline{y}$ = ln 8 to give $\dot{Q}_P$ = 5.95 l/s and $\dot{Q}_S$ = 0. The second case had identical parameters, except $\overline{y}$ = ln 10 to give $\dot{Q}_P$ = 4.76 l/s, together with a 15% shunt, $\dot{Q}_S$ = 0.84 l/s. In each case, the retentions over the course of a series of whole breaths were recorded. We begin by considering

the highest and lowest retentions over the course of a breath. We then consider two time-averaged cases. First, using *Eq. 19,* we time average the retentions over the course of a whole breath. Second, we time average over an interval containing two troughs of retentions (Fig. 1). Suppose a breath starts at *time t_j.* Then, using *Eq. 19,* we take a time average of retentions over the interval $t_j + \tau_0 < t < t_j + \tau_1$, where $\tau_0 = 0.518$ s and $\tau_1 = 7.317$ s. This gives a time interval of 6–7 s, a feasible interval in which to take a blood sample. We justify taking this particular interval later.

One-compartment model. Although the retentions were generated using a unimodal distribution, because of the large fluctuations in retentions over the course of a breath, as seen in Fig. 1, we do not assume that the
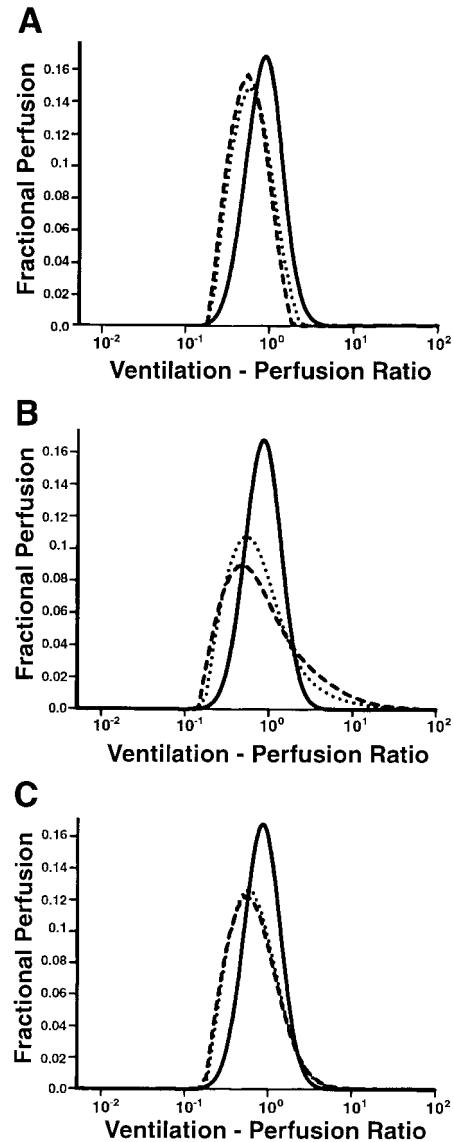
Fig. 3. Given ventilation-perfusion distribution (solid line) and distributions recovered using 50-compartment model with use of retentions generated with end-expiratory alveolar volume of 1,700 ml (dashed line) and end-expiratory alveolar volume of 3,400 ml (dotted line). *A*: distributions recovered when highest retentions are used; *B*: distributions recovered when lowest retentions are used; *C*: distributions recovered when time-averaged retentions are used.

Table 3. *Differences in retention caused by varying widths of ventilation-volume distribution*

Partition Coefficient	Retention					
	Set $R_{1,L}$	$R_{1,H}$	Set $\overline{R}_1$	Set $R_{2,L}$	Set $R_{2,H}$	Set $\overline{R}_2$
5.99×10^{-3}	0.0071	0.0080	0.0076	0.0070	0.0080	0.0075
8.56×10^{-2}	0.0922	0.1040	0.0982	0.0910	0.1037	0.0975
5.35×10^{-1}	0.3796	0.4282	0.4045	0.3761	0.4282	0.4032
2.34	0.7001	0.7893	0.7474	0.6939	0.7886	0.7451
12.5	0.8766	0.9789	0.9399	0.8706	0.9751	0.9366
2.85×10^2	0.9863	1.0000	0.9970	0.9829	0.9966	0.9936

In 1st 3 sets of retention ($R_{1,L}$, $R_{1,H}$, and $\overline{R}_1$), $\sigma_x = 0.0625$; in 2nd 3 ($R_{2,L}$, $R_{2,H}$, and $\overline{R}_2$), $\sigma_x = 0.5$. Subscripts H and L refer to highest and lowest retentions over course of a breath; $\overline{R}_1$ and $\overline{R}_1$ refer to retentions that are time averaged over a whole breath.

recovered nontidal model will be unimodal. Instead, we used a two-compartment model recovery process. However, for all the retentions considered, the recovered distribution had one compartment with zero perfusion, and so the recovered distribution was unimodal, and an estimate for shunt fraction and $\dot{V}/\dot{Q}$ ratio of the ventilated compartment was given. These parameters, recovered using the highest retentions, the lowest retentions, and the retentions time averaged over a whole breath, are shown in Table 4.

The shunt fractions recovered in Table 4 are of acceptable clinical accuracy. Shunt is mainly determined by the least soluble gas. We saw in Fig. 1 that the retention of this gas ($\lambda = 5.99 \times 10^{-3}$) hardly varied at all over the course of each breath, and so the estimation of shunt is relatively unaffected by the tidal nature of breathing.

The values of $\dot{V}/\dot{Q}$ ratios recovered vary depending on when the arterial blood is sampled during the respiratory cycle. If the lowest retentions are used, then in this (standard) case, there is a 77% higher estimation of $\dot{V}/\dot{Q}$ ratio than would be estimated using the highest retentions. Even in practice, where the time-averaged retentions would be used, the value of the $\dot{V}/\dot{Q}$ ratio recovered is inaccurate.

Fifty-compartment models. EFFECT OF ASSUMING CONTINUOUS VENTILATION IN THE PARAMETER RECOVERY ROUTINE. The retentions described above were given to the recovery process for the 50-compartment model. The distributions recovered using the highest and lowest retentions over the course of a breath are shown in Fig. 4A for zero shunt and Fig. 4B for 15% shunt. Also

Table 4. *$\dot{Q}s/\dot{Q}_T$ and $\dot{V}/\dot{Q}$ ratios recovered using generated retentions from one-compartment model*

Retention	Given Shunt = 0		Given Shunt = 15%	
	$\dot{Q}s/\dot{Q}_T$	$\dot{V}/\dot{Q}$	$\dot{Q}s/\dot{Q}_T$	$\dot{V}/\dot{Q}$
High	0.000	0.782	0.148	0.972
Low	0.022	1.388	0.168	1.715
Avg	0.007	0.991	0.156	1.235

$\dot{Q}s/\dot{Q}_T$, shunt fraction; $\dot{V}/\dot{Q}$, ventilation-perfusion; high, highest retentions over course of a breath; low, lowest retentions. When given shunt = 0, true value of $\dot{V}/\dot{Q} = 1.109$; when given shunt = 15%, true value of $\dot{V}/\dot{Q} = 1.387$.
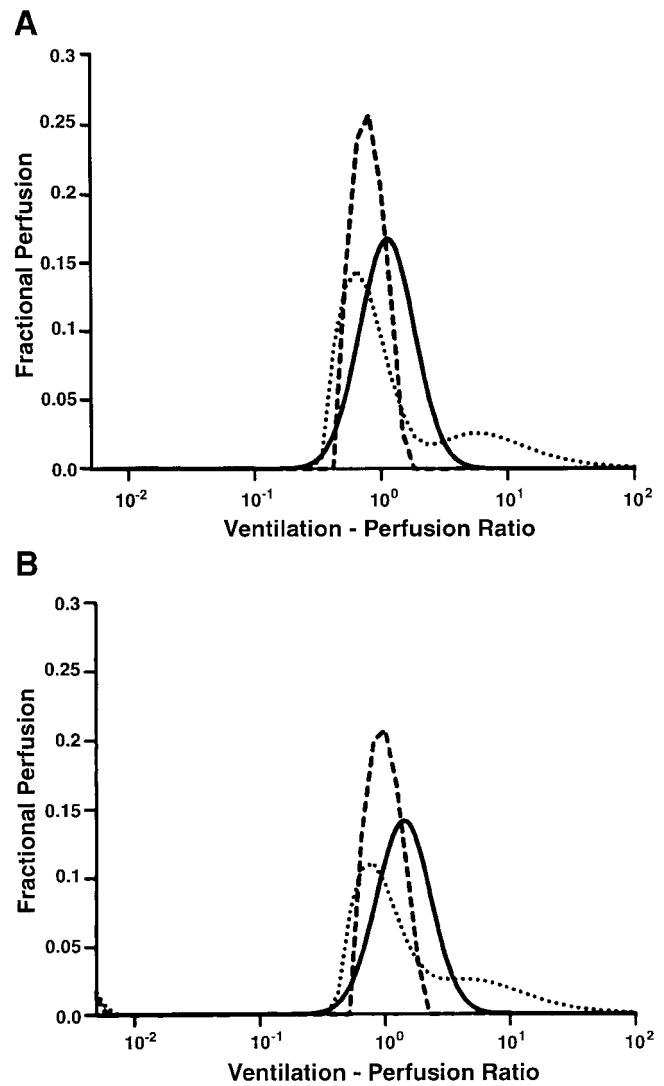

Fig. 4. Ventilation-perfusion distributions generated using retentions at different stages of a single breath. *A*: data generated with no shunt; *B*: data generated with 15% shunt. Solid lines, given distribution; dashed lines, distribution recovered when highest retentions measured are used; dotted lines, distribution recovered when lowest retentions measured are used (see Fig. 1 for a whole breath).

shown is the given $\dot{V}/\dot{Q}$ distribution. This allows us to consider the effect of substituting tidally generated data into a parameter recovery routine that assumes continuous ventilation. The recovered distributions in each plot are quite different. The highest retentions give a narrow, unimodal distribution that is narrower and higher than the given distribution and has a peak that is at a lower $\dot{V}/\dot{Q}$ ratio than the given distribution; the lowest retentions give a bimodal distribution. This bimodal distribution has one mode of approximately the correct width in the same position as the unimodal distribution seen for the highest retentions, together with a spurious, broad distribution of compartments with high $\dot{V}/\dot{Q}$ ratios. As a result, we become wary of any set of retentions that are time averaged in such a way as to be weighted toward the troughs seen in Fig. 1. This is why we have chosen our τ_0 and τ_1 to take the values chosen. The retentions are now averaged over

two troughs of retentions and the portion of the breath between the troughs.

EFFECT OF DIFFERENT SAMPLING INTERVALS. The distributions recovered using the time-averaged retentions are shown in Fig. 5A for zero shunt and Fig. 5B for 15% shunt. The given distributions, the distributions recovered when the retentions are averaged over the course of a whole breath, and the distributions recovered when the retentions are averaged over the time interval $t_j + \tau_0 < t < t_j + \tau_1$ described above are shown. This allows us to investigate the effect of different experimental sampling intervals on the recovered distributions. Both ways of time averaging the retentions lead to distributions skewed to the right and a mode with a peak to the left of the peak of the given distribution. However, the retentions that are time averaged over the interval $t_j + \tau_0 < t < t_j + \tau_1$ give a more highly skewed distribution
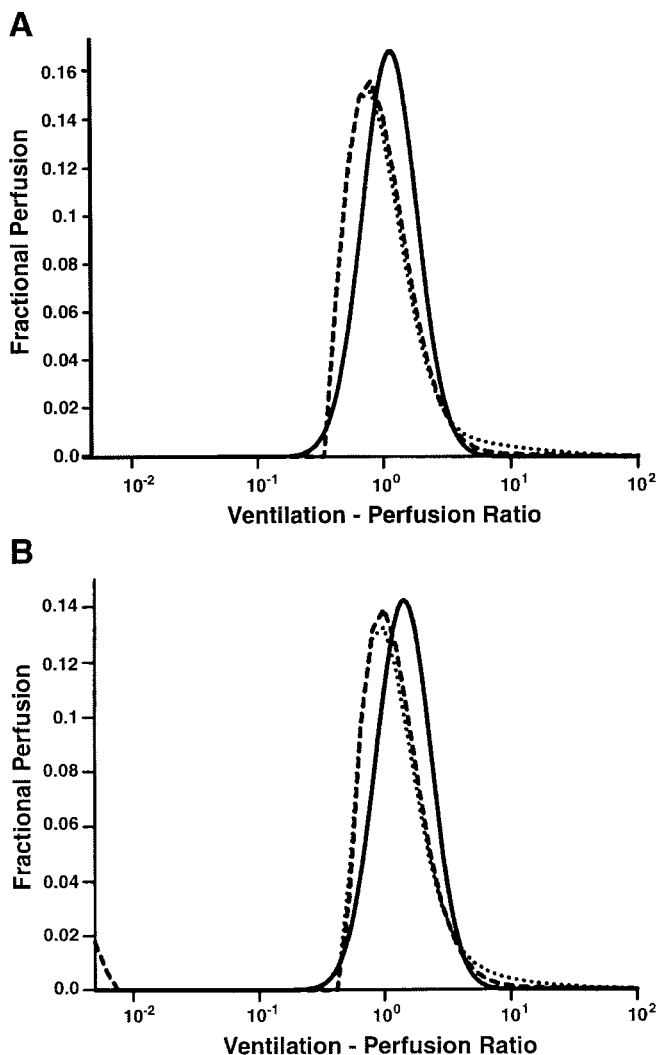

Fig. 5. Ventilation-perfusion distributions generated using retentions averaged over different time intervals. *A*: data generated with no shunt; *B*: data generated with 15% shunt. Solid lines, given distribution; dashed lines, distribution recovered when retentions are averaged over a whole breath (i.e., arterial blood samples are drawn over a whole breath time interval, 5 s in this example); dotted lines, distribution recovered when retentions are measured over a portion of 2 breaths (see RESULTS for details).

that includes compartments with higher $\dot{V}/\dot{Q}$ ratios. Withdrawing an arterial blood sample over a period of time that is an integer multiple of the breath length will ensure that the retentions are representative of the whole breathing cycle and that there is no weighting of these retentions toward the troughs of the retentions shown in Fig. 1.

DISCUSSION

We have demonstrated using a mathematical model that the intrabreath fluctuations in retention, caused by the nature of tidal breathing, are significant in the parameter recovery process and that the simpler continuous ventilation models previously used (2, 11) must be used with care. Although the tidal breathing model is a more physically realistic model than the continuous ventilation model, it must be remembered that we have assumed a uniform filling and emptying of all compartments when deriving the conservation of mass equations. It is unlikely that this would be true in a patient with pulmonary dysfunction.

We generated retentions using a standard lung with unimodal $\dot{V}/\dot{Q}$ and $\dot{V}A/\dot{V}A$ distributions. When a tidal breathing model is used, it was shown that the retentions vary with time. There is a variation of ~20% in some cases considered here. We would normally expect that experimental data would be correct to within 3% of the mean concentration of each gas (10), and so the variations in the inert gas retentions within each breath should warn us to expect differences in recovered parameters, depending on the time at which the arterial blood is sampled during the respiratory cycle.

We have shown that we can indeed recover widely varying parameters when using retentions at different points of the breath. Most notable is the recovery of a bimodal distribution by the 50-compartment lung model when the given distribution is truly unimodal when the lowest set of retentions over the course of a breath is used. However, this problem can be avoided to a large extent by the physical necessity of taking time-averaged blood samples, and we have shown that the blood sample used to measure the retentions should be taken over the course of a series of whole breaths to avoid weighting toward the troughs in retentions seen in Fig. 1. Even so, in the cases that we have considered, this resulted in a distribution skewed to the right and with the peak shifted to the left of the given distribution. We have also shown that the one-compartment model, although it correctly recovered a unimodal distribution, recovers parameters varying by up to 80%, so this model is not a practical alternative to the 50-compartment model.

Our final aim in this study was to investigate the effect of $\dot{V}A/\dot{V}A$ distribution on the retentions generated. We used log-normal functions of the $\dot{V}A/\dot{V}A$ ratio and showed that the width of the distribution had a negligible effect on the retentions. However, the VA_T could change the retentions by an amount greater than that expected due to experimental error. A higher alveolar volume had the effect of moving the distribution toward higher $\dot{V}/\dot{Q}$ ratios.

We conclude by stating that if MIGET is to be used, then the retentions should be time averaged over the course of a series of whole breaths. This will minimize the effects of tidal breathing on the experimental data.

REFERENCES

1. **Evans, J. W., and P. D. Wagner.** Limits on $\dot{V}A/\dot{Q}$ distributions from analysis of experimental inert gas elimination. *J. Appl. Physiol.* 42: 889–898, 1977.
2. **Farhi, L. E.** Elimination of inert gas by the lung. *Respir. Physiol.* 3: 1–11, 1967.
3. **Farhi, L. E., and T. Yokoyama.** Effects of ventilation-perfusion inequality on elimination of inert gases. *Respir. Physiol.* 3: 12–20, 1967.
4. **Gavaghan, D. J., and C. E. W. Hahn.** A tidal breathing model of the forced inspired inert gas sinewave technique. *Respir. Physiol.* 106: 209–221, 1996.
5. **Kapitan, K. S., and P. D. Wagner.** Linear programming analysis of $\dot{V}A/\dot{Q}$ distributions: limits on central moments. *J. Appl. Physiol.* 60: 1772–1781, 1986.
6. **Mitchell, R. R., R. M. Wilson, and D. Sierra.** ICU monitoring of ventilation distribution. *Int. J. Clin. Monit. Comput.* 2: 199–206, 1986.
7. *NAG Fortran Library Manual-Mark 14.* Oxford, UK: Numerical Algorithms Group, 1990.
8. **Ratner, E. R., and P. D. Wagner.** Resolution of the multiple inert gas method for estimating $\dot{V}A/\dot{Q}$ maldistribution. *Respir. Physiol.* 49: 293–313, 1982.
9. **Stewart, W. E., and S. M. Mastenbrook, Jr.** Parametric estimation of ventilation-perfusion ratio distributions. *J. Appl. Physiol.* 55: 37–51, 1983.
10. **Wagner, P. D., P. F. Naumann, and R. B. Laravuso.** Simultaneous measurement of eight foreign gases in blood by gas chromatography. *J. Appl. Physiol.* 36: 600–605, 1974.
11. **Wagner, P. D., H. A. Saltzman, and J. B. West.** Measurement of continuous distributions of ventilation-perfusion ratios: theory. *J. Appl. Physiol.* 36: 588–599, 1974.